

# Enhanced morphological stability of silver nanoparticles supported on rough substrates at high temperatures

Ryan D. Scherzer<sup>1</sup>, Lev V. Gasparov<sup>2</sup>, Stephen P. Stagon<sup>1</sup> ✉

<sup>1</sup>Mechanical Engineering Department, University of North Florida, Jacksonville, Florida, 32224, USA

<sup>2</sup>Physics Department, University of North Florida, Jacksonville, Florida, 32224, USA

✉ E-mail: s.stagon@unf.edu

Published in *Micro & Nano Letters*; Received on 18th July 2017; Revised on 12th December 2017; Accepted on 22nd December 2017

Noble metal nanostructures serve as excellent substrates for the detection of trace amounts of substances in surface enhanced Raman spectroscopy, but they have not found widespread commercial use due to their instability and short shelf lives. This work demonstrates that silver nanoparticles grown onto substrates with nanoscale roughness, using glancing angle physical vapour deposition and subsequently thermally annealed at 500°C to generate a stable lower energy configuration, exhibit Raman enhancements that are strong and remain stable with no drop over 30 days. These nanoparticle arrays may serve as time stable substrates for commercial scale Raman spectroscopy or may be employed in harsh environments.

**1. Introduction:** Noble metal nanostructures, like nanorods and nanoparticles, are particularly useful for sensing applications due to their unique optical properties, particularly surface plasmon resonance [1–11]. For example, silver (Ag) nanorods grown using physical vapour deposition (PVD) exhibit very large enhancement of the Raman signal when used as a substrate for surface enhanced Raman spectroscopy (SERS) [7–10]. While there is tremendous promise for the widespread commercial use of portable Raman sensing platforms and low cost mass produced SERS substrates, this has not yet materialised due at least in part to the instability of the substrates [11–13]. The instability of the substrates has been shown to derive from chemical and physical origins. The chemical and physical instability are largely coupled, with the surface chemical termination having an impact on the surface diffusivity of atoms [12]. For the case of Ag, the high diffusivity of atoms on the surface gives rise to rapid surface diffusion at low temperatures, which leads to the reshaping of the nanostructure driving coarsening towards bulk and loss of Raman signal enhancement [11–13]. Interestingly, for the case of Ag, the stable oxide species, Ag<sub>2</sub>O, has a significantly lower melting temperature than pure Ag, and therefore may even act to speed up diffusion and the ensuing coarsening [14].

With the goal of designing a means of stopping coarsening and loss of the Raman signal, we first examine the steps of the coarsening mechanism. The physical mechanism of coarsening for nanorods and nanoparticles is similar. First, thermally driven surface diffusion leads to reshaping of the nanostructures [11, 12, 15]. As the structures are so close to one another on their base substrate, they touch with their neighbour, leading to bridging and eventual ripening of multiple rods or particles into one with a diameter approaching bulk [12, 13].

Several methods have been previously reported in the literature to stop the rapid coarsening, and these methods primarily rely on capping the nanostructures with a high melting temperature material to stop diffusion [13, 16, 17]. For example, an oxide cap has been deposited on the top of Ag nanorods and has been shown to prevent surface diffusion effectively up to temperatures of 350°C [13, 17]. Unfortunately, any sort of cap creates a barrier between the nanostructure and the substance to be detected by SERS, and the Raman enhancement drops significantly [13].

In this Letter, we present a method of creating a stable array of Ag nanoparticles, which demonstrate exceptional Raman enhancement stability after exposure to elevated temperatures and over time,

by using a substrate with high nanoscale roughness to first seed deposition and then slow diffusion of Ag deposited onto its surface. Through thermal annealing, the Ag shapes relax to lower energy configurations, and when returned to room temperature the samples exhibit stable morphology and Raman enhancement for over one month.

**2. Experimental methods:** Before presenting the results, we briefly describe the experimental methods of fabrication and characterisation. Substrates with nanoscale seeds are created through PVD deposition of aluminium (Al) metal onto fused silica slides with subsequent thermal annealing in air. First, the fused silica slides are ultrasonically cleaned using acetone, ethanol, and deionised water and are allowed to air dry. The samples are then mounted into a glancing angle deposition thermal evaporation PVD system at an incident angle of 87° [18]. The base pressure of the system is  $6 \times 10^{-4}$  Pa and the working pressure is  $\sim 6 \times 10^{-3}$  Pa. Al source material (99.95% Kurt J. Lesker Co.) is then deposited to a thickness of 50 nm at a deposition rate of 0.3 nm/s, measured perpendicular to the flux using a quartz crystal microbalance. After growth, the samples are removed and heated in air at 500°C for 24 h in the air and the colour is observed to change from metallic grey to clear over this time. After cooling to room temperature, the samples are then placed back into the PVD system and Ag (99.995% Kurt J. Lesker Co.) is deposited at the same glancing angle to thicknesses ranging from 25 to 100 nm at a rate of 0.5 nm/s. Immediately the following deposition, samples are annealed in air at temperatures of  $500^\circ\text{C} \pm 25^\circ$  to  $750^\circ\text{C} \pm 37.5^\circ$  for time durations of 10 min, 1 h, and 48 h, respectively. Ultraviolet-visible spectroscopy (UV-vis) is performed on all of the samples using a Perkin Elmer Lambda 35 operating over a range of 200–700 nm, with 1 nm spectral slit bandwidth, at a scan speed of 480 nm/min. Scanning electron microscopy (SEM) is performed using an FEI Nova Nano microscope operating at 15.0 kV using the through-lens secondary electron detector. Particle size distribution is analysed using ImageJ by thresholding images, calculating the number of pixels per particle for each case, and estimating the diameter of each of the particles based on the approximation that each particle is roughly circular. Finally, Raman spectroscopy is performed by detecting aqueous  $1 \times 10^{-6}$  M rhodamine 6 g (R6G) (Sigma Aldrich Co.) using a Horiba T64000 Raman Spectrometer equipped with the microscope utility and liquid nitrogen cooled CCD detector.  $10\times$  Olympus objectives focused 532 nm excitation laser in  $\sim 10 \mu\text{s}$  spot on the surface of the

sample. The laser power did not exceed  $10 \mu\text{W}$ . We used the spectrometer in the ‘direct mode’ by bypassing the pre-monochromator and sending the scattered light directly to the spectrograph equipped with 600 lines/mm holographic grating. Kaiser Optics super notch filter suppressed the intensity of the laser line. The entrance slit of the spectrometer was set at  $200 \mu\text{m}$ . The accumulation time was set at 1 s with 25 accumulations per spectrum. The spectral range extended from 250 to 2250 wavenumbers.

**3. Results and discussion:** Building from the bottom up, we first present the morphology and optical absorption of the nanostructured substrate, as shown in Fig. 1. The purpose of the roughness of the substrate is to initiate the growth of small Ag clusters with large spacing between clusters and to provide a torturous surface for long range diffusion and coarsening. Through the thermal annealing in air, the Al present has fully reacted to form a transparent oxide. We also note that the substrate is nearly optically transparent in the visible spectrum and should not contribute to the Raman signal and may be useful for optical sensing techniques.

Next, we present the structures that result in deposition of 25 nm of Ag and subsequent thermal annealing in air. As fabricated, the Ag has coated the high spots of the rough substrate, and the clusters are numerous and  $<50 \text{ nm}$  in diameter, inset Fig. 2a.

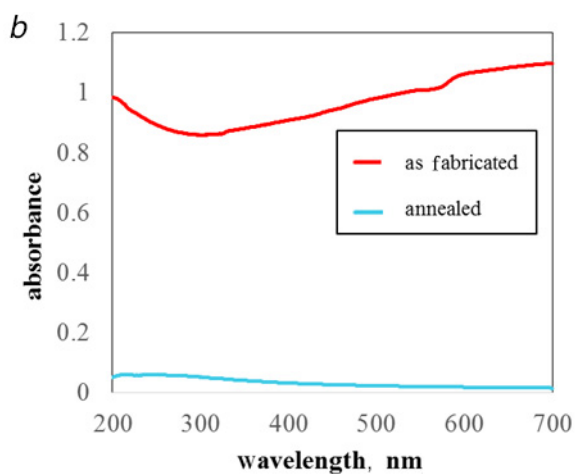
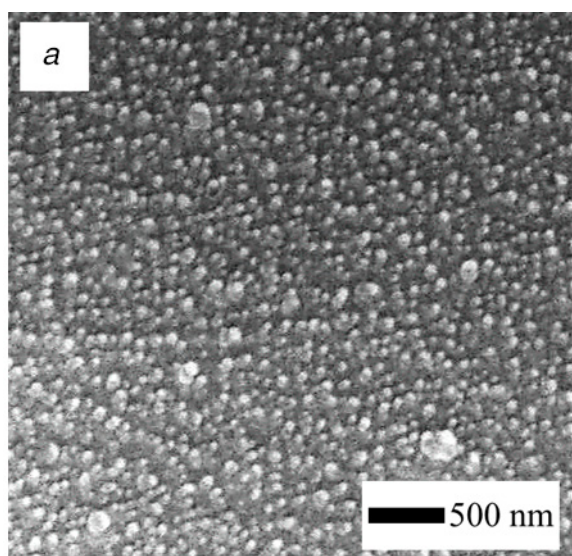


**Fig. 1** Rough nanostructured substrate created through the thermal annealing of 50 nm Al seeds  
*a* SEM micrograph of the created substrate, with  $<3 \text{ nm}$  of gold sputtered onto the surface with rotation for SEM imaging and  
*b* UV-vis spectra of the substrate before and after annealing

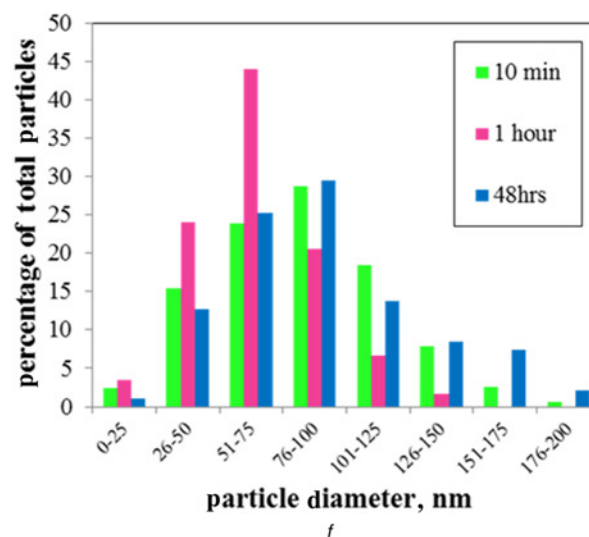
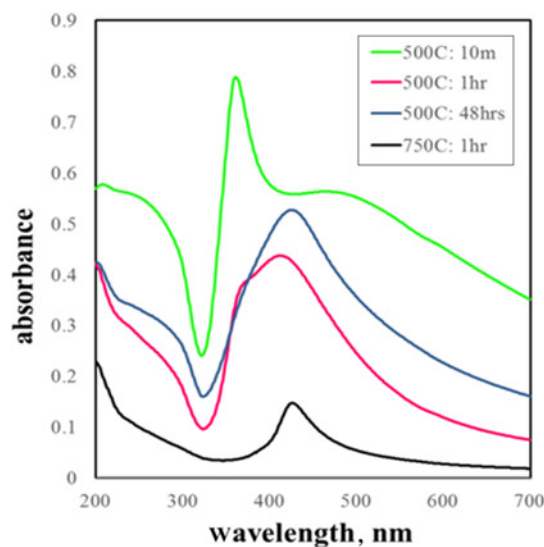
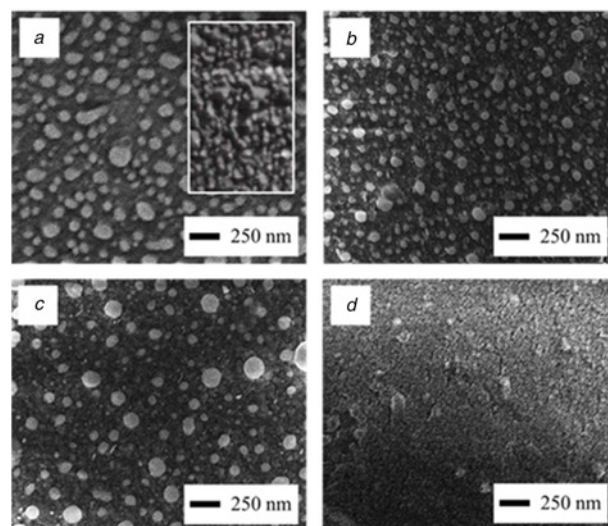


**Fig. 2** Stable Ag nanoparticles: SEM micrographs of the nanoparticles at the annealing conditions of  
*a* 500°C for 10 min  
*b* 500°C for 1 h  
*c* 500°C for 48 h, and  
*d* 750°C for 1 h  
*e* Accompanying optical absorbance measurements  
*f* Histogram of particle diameter distribution

Next, we anneal the sample at 500°C to allow for thermal diffusion to take place and to drive the shapes of the particles to a lower energy configuration. After annealing in air for 10 min, the nanoparticles have coarsened but still remain small with average diameters of 91 nm, as shown in Fig. 2a. Next we push the annealing time and temperature even further to test the thermal stability of our samples for applications in very harsh environments. When annealing is instead held for 1, as shown in Fig. 2b, further diffusion is evident, giving rise to an average diameter 69 nm, but with a larger standard deviation than in Fig. 2a. Some of the larger particles may have sufficient thermal energy to split and diffuse long distances on the substrate. After annealing for 48 h, more mobility and subsequent coarsening are evident, with an average diameter increasing to 98 nm, as shown in Fig. 2c. As a test of the upper level of stability, the sample is heated to 750°C, and it is evident that the Ag has reacted with the underlying substrate and atmosphere and is no longer nanoparticles, as shown in Fig. 2d. The authors suggest that when heated, small Ag particles, within a range of ~200 nm, are able to diffuse and reach one another to the bridge, coarsening to generate larger particles. The roughness of the substrate then prevents these larger particles from translating far enough to join together and coarsen to bulk. This excellent thermal stability at elevated

temperatures should lead to long term morphological stability when the samples are returned to room temperature. Optical absorption measurements in Fig. 2e show that the width, intensity, and position of the absorption peak shift after thermal annealing. The samples annealed for only 10 min exhibit a strong and narrow absorption peak centred ~350 nm indicative of surface plasmon resonance, while those annealed for longer show peak broadening and red shifting towards ~450 nm, which may be attributed to a larger spread in diameters of the particles. Fig. 2f shows a histogram, graphically representing the spread of particle diameters for the three heating cases shown in 2a–c, respectively. The variance in the particle diameter distribution shown in Fig. 2f coupled with chemical changes to the surfaces of the Ag nanoparticles due to annealing in air result in the observed changes in optical absorption of Fig. 2e. The authors note that the presence of oxide on the surface of the Ag nanoparticles is unlikely as the dominant oxide species of Ag, Ag<sub>2</sub>O, and Ag<sub>2</sub>O<sub>2</sub>, are both thermally unstable above 400°C and decompose [19]. Additionally, a recent study has demonstrated that Ag nanostructures of similar dimension require exposure in ambient for ~100 days before oxidation is observed to take place [20].

Putting the structure to the test, we next present the Raman enhancement of the samples and test their stability in air, as shown in Fig. 3. Compared to the as-fabricated unheated sample, the normalised Raman signal of the sample that was annealed for 10 min at 500°C remains strong, and has a similar signal to noise ratio, as shown in Fig. 3a. Normalisation is performed for each data set to the largest raw count value of that particular set to isolate and compare the signal-to-noise ratio of the different samples. A shift in relative peak intensities can be attributed to some reaction with the atmosphere and the substantial morphology change. When stored in air for over 30 days, the normalised intensity of the representative peak at 765 cm<sup>-1</sup> remains nearly unchanged, with a scatter representative of variation from measuring at different spots on the same substrate. Normalisation is performed to the maximum raw counts peak in each data set to highlight the comparable signal-to-background ratio of the samples, rather than raw counts. In comparison, Ag nanorods decrease to 4% of their original enhancement over 30 days in the air [21]. Further, when the morphology of our samples after 30 days is investigated using SEM the mean particle diameter is within 5% of the original diameter, which is within the spot-to-spot spread on a single substrate.

**4. Conclusion:** In this Letter, we demonstrate the use of a rough nanostructured substrate to increase the morphological stability of Ag nanoparticles grown using PVD. By heating to 500°C in air, the deposited nanoparticles transition to a state of higher stability, but remain nano with a diameter of <100 nm and exhibit strong absorption of visible light. The samples exhibit strong Raman enhancement, here using R6G as a prototype molecule to detect, and the enhancement remains nearly constant for over 30 days. These samples may serve as a time stable substrate for Raman spectroscopy, which can be stored in ambient without a reduction in Raman enhancement, or could be used in high temperature sensing applications.

**5. Acknowledgments:** The authors acknowledge the financial support of the National Aeronautics & Space Administration through the University of Central Florida's NASA Florida Space Grant Consortium and Space Florida. LVG acknowledges the support by the University of North Florida's Terry Presidential Professorship and Office of Naval Research grant no. N00014-06-1-0133.

## 6 References

- [1] Moskovits M.: 'Surface-enhanced spectroscopy', *Rev. Mod. Phys.*, 1985, **57**, pp. 783–823

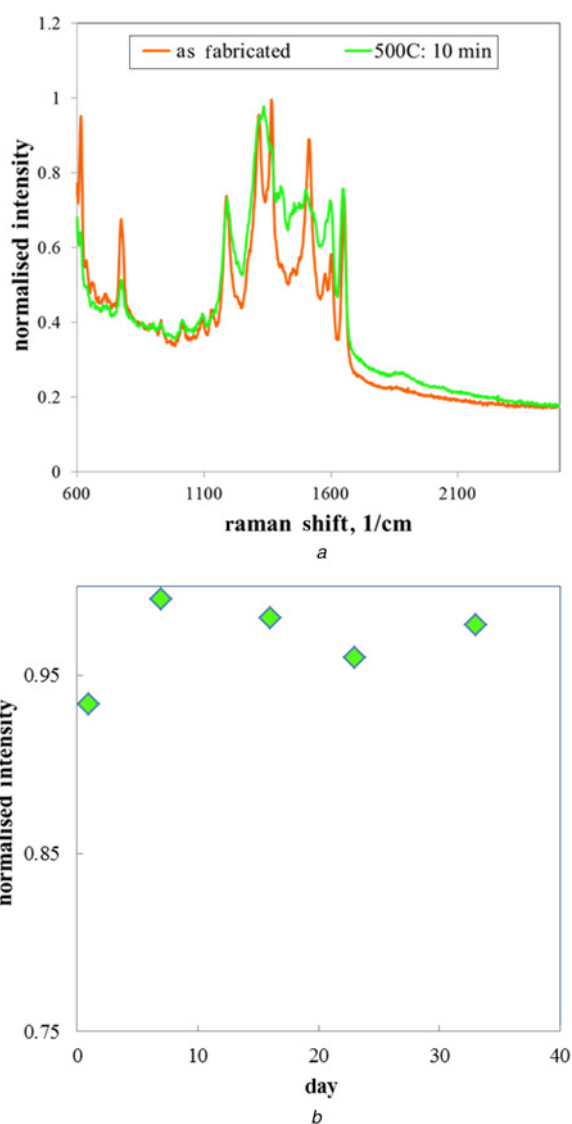


**Fig. 3 Raman spectroscopy**  
a Raman spectroscopy of R6G on the substrates before and after annealing for 10 min at 500°C and  
b Normalised intensity of the Raman peak at 765 cm<sup>-1</sup> versus days in air

- [2] Eustis S., El-Sayed M.A.: 'Why gold nanoparticles are more precious than pretty gold: noble metal surface plasmon resonance and its enhancement of the radiative and nonradiative properties of nanocrystals of different shapes', *Chem. Soc. Rev.*, 2006, **35**, pp. 209–217
- [3] Anker J.N., Hall W.P., Lyandres O., *ET AL.*: 'Biosensing with plasmonic nanosensors', *Nat. Mater.*, 2008, **7**, pp. 442–453
- [4] Shanmukh S., Jones L., Driskell J., *ET AL.*: 'Rapid and sensitive detection of respiratory virus molecular signatures using a silver nanorod array SERS substrate', *Nano Lett.*, 2006, **6**, pp. 2630–2636
- [5] Qian X.M., Nie S.M.: 'Single-molecule and single-nanoparticle SERS: from fundamental mechanisms to biomedical applications', *Chem. Soc. Rev.*, 2008, **37**, pp. 912–920
- [6] Sun X., Stagon S.P., Huang H.C., *ET AL.*: 'Functionalized aligned silver nanorod arrays for glucose sensing through surface enhanced Raman scattering', *RCS Adv.*, 2014, **4**, pp. 23382–23388
- [7] Chaney S.B., Shanmukh S., Dluhy R.A., *ET AL.*: 'Aligned silver nanorod arrays produce high sensitivity surface-enhanced Raman spectroscopy substrates', *Appl. Phys. Lett.*, 2005, **87**, p. 031908
- [8] Cañamares M.V., Garcia-Ramos J.V., Gómez-Varga J.D., *ET AL.*: 'Comparative study of the morphology, aggregation, adherence to glass, and surface-enhanced Raman scattering activity of silver nanoparticles prepared by chemical reduction of Ag<sup>+</sup> using citrate and hydroxylamine', *Langmuir*, 2005, **21**, pp. 8546–8553
- [9] Goel P., Singh J.P.: 'Fabrication of silver nanorods embedded in PDMS film and its application for strain sensing', *J. Phys. D, Appl. Phys.*, 2015, **48**, (44), p. 445303
- [10] Kumar S., Goel P., Singh J.P.: 'Flexible and robust SERS active substrates for conformal rapid detection of pesticide residues from fruits', *Sens. Actuators B, Chem.*, 2017, **241**, pp. 577–583
- [11] Stagon S, Huang H.: 'Airtight metallic sealing at room temperature under small mechanical pressure', *Sci. Rep.*, 2013, **3**, p. 3066
- [12] Beavers K.R., Marotta N.E., Bottomley L.A.: 'Thermal stability of silver nanorod arrays', *Chem. Mater.*, 2010, **22**, pp. 2184–2189
- [13] Bachenheimer L., Elliot P., Stagon S., *ET AL.*: 'Enhanced thermal stability of Ag nanorods through capping', *Appl. Phys. Lett.*, 2014, **105**, p. 213104
- [14] Assal J., Hallstedt B., Gauckler L.J.: 'Thermodynamic assessment of the silver–oxygen system', *J. Am. Ceram. Soc.*, 1997, **80**, (12), pp. 3054–3060
- [15] Li Y., Wu Y., Ong B.S.: 'Facile synthesis of silver nanoparticles useful for fabrication of high-conductivity elements for printed electronics', *J. Am. Chem. Soc.*, 2005, **127**, pp. 3266–3267
- [16] Ma L., Huang Y., Hou M., *ET AL.*: 'Ag nanorods coated with ultrathin TiO<sub>2</sub> shells as stable and recyclable SERS substrates', *Sci. Rep.*, 2015, **5**, p. 15442
- [17] John J.F., Mahurin S., Dai S., *ET AL.*: 'Use of atomic layer deposition to improve the stability of silver substrates for in situ, high temperature SERS measurements', *J. Raman Spectrosc.*, 2010, **41**, pp. 4–11
- [18] Robbie K., Brett M.J.: 'Sculptured thin films and glancing angle deposition: growth mechanics and applications', *J. Vac. Sci. Technol. A*, 1997, **15**, pp. 1460–1465
- [19] Waterhouse G.I., Bowmaker G.A., Metson J.B.: 'The thermal decomposition of silver (I, III) oxide: a combined XRD, FT-IR and Raman spectroscopic study', *Phys. Chem. Chem. Phys.*, 2001, **3**, (17), pp. 3838–3845
- [20] Huang H., Gasparov L., Bachenheimer L., *ET AL.*: 'Degradation mechanism of Ag nanorods for surface enhanced Raman spectroscopy', *Sci. Rep.*, 2017, **7**, p. 16282
- [21] Nuntawong N., Eiamchai P., Wong-ek B., *ET AL.*: 'Shelf time effect on SERS effectiveness of silver nanorod prepared by OAD technique', *Vacuum*, 2013, **88**, pp. 23–27